A GPR-Protein Interaction Surface of Giα: Implications for the Mechanism of GDP-Release Inhibition†

Michael Natochin,‡ Karim G. Gasimov, and Nikolai O. Artemyev*,§

Department of Physiology and Biophysics, University of Iowa College of Medicine, Iowa City, Iowa 52242

Received August 22, 2001; Revised Manuscript Received November 8, 2001

ABSTRACT: Proteins containing G-protein regulatory (GPR) motifs represent a novel family of guanine nucleotide dissociation inhibitors (GDIs) for Gα subunits from the Gi family. They selectively interact with the GDP-bound conformation of Giα and transducin-α (Gtα), but not with Gsα. A series of chimeric proteins between $Gi\alpha_1$ and Gsα has been constructed to investigate GPR-contact sites on Gα subunits and the mechanism of GPR-protein GDI activity. Analysis of the interaction of two GPR-proteins—AGS3GPR and Pcp2—with the chimeric Gα subunits demonstrated that the GPR−$Gi\alpha_1$ interface involves the $Gi\alpha_1$ switch regions and $Gi\alpha_1$-144−151, a site within the helical domain. Residues within $Gi\alpha_1$-144−151 form conformation-sensitive contacts with switch III, and may directly interact with a GPR-protein or form a GPR-binding surface jointly with switch III. The helical domain site is critical to the ability of GPR-proteins to act as GDIs. Our data suggest that a mechanism of the GDI activity of GPR-proteins is different from that of GDIs for monomeric GTPases and from the GDI-like activity of G$\beta\gamma$ subunits. The GPR-proteins are likely to block a GDP-escape route on Gα subunits.

Heterotrimeric G-proteins (G-proteins) transduce a multitude of extracellular signals that activate G-protein coupled receptors (GPCRs).[1] The mechanisms of G-protein signaling regulation are numerous and complex (*1*−*4*). Recently, a novel group of G-protein modulators has been recognized (*5*−*7*). These G-protein modulators share conserved sequence repeats named the G-protein regulatory (GPR) (*5*) or GoLOCO motifs (*6*). Several characterized GPR-proteins, AGS3, LGN, Pcp2, and Rap1GAP, show selective high-affinity binding to Giα and transducin-α (Gtα), whereas the interaction with Goα is weaker (*8*−*12*). No interaction between a GPR-protein and Gsα has been detected (*9*−*11*). GPR-proteins preferentially recognize the GDP-bound conformations of Giα-like Gα subunits. The binding of GPR-proteins to GαGDP is competitive with G$\beta\gamma$ binding, suggesting overlapping interaction sites (*10*, *11*). The functional significance of the GPR-protein/Gα interaction remained unclear until recently, when AGS3 was found to inhibit GDP release and GDP/GTP exchange of Giα (*8*, *9*). Furthermore, AGS3 was capable of inhibiting rhodopsin-stimulated activation of transducin (*9*). Subsequently, other GPR-motif containing proteins—LGN, Pcp2, Rap1GAP, and RGS12/14—have been shown to act as the guanine nucleotide dissociation inhibitors (GDIs) toward Giα (*11*, *13*). These findings underscored a potential physiological role of GPR-proteins as the first known family of GDI for heterotrimeric G-proteins. The GPR-contact sites on Gα subunits and the mechanism of GDI activity have not yet been elucidated. In this study, we constructed a number of chimeric Gα subunits between Giα and Gsα. Two GPR-proteins, Pcp2 and the GPR-domain of AGS3 (AGS3GPR), have been analyzed for their ability to bind to and inhibit nucleotide exchange on Giα/Gsα chimeras. Our results suggest a mechanism of the GDI activity of GPR-proteins.

EXPERIMENTAL PROCEDURES

Materials. [^{35}S]GTPγS (1160 Ci/mmol) was purchased from Amersham Pharmacia Biotech. Restriction enzymes were from New England Biolabs. T4 DNA ligase was from Roche Molecular Biochemicals. Cloned *Pfu* DNA polymerase was from Stratagene. L-1-Tosylamido-2-phenylethyl chloromethyl ketone-treated trypsin was from Worthington. 3-(Bromoacetyl)-7-diethylaminocoumarin (BC) was from Molecular Probes. Glutathione−agarose was from Sigma. *E. coli* strain DH5αF′ was from Life Technologies, Inc. Dam$^-$/Dcm$^-$ strain GM2163 was from New England Biolabs. BL21(DE3) strain was from Novagen. Other reagents were from Sigma or Fisher.

Preparation of Chimeric Gα Subunits. The rat $Gi\alpha_1$ and short splice bovine Gsα cDNAs subcloned using the *Nco*I and *Hin*dIII restriction sites into the $pHis_6$ vector (*14*, *15*) were used for the construction of chimeric Giα/Gsα. The numbering for the long splice form Gsα is used throughout the text for clarity. Three unique silent restriction sites were

† This work was supported by National Institutes of Health Grant RO1 EY-12682 and American Heart Association Grant 0140195N. NIH Grant DK-25295 supported the services provided by the Diabetes and Endocrinology Research Center of the University of Iowa.

* To whom correspondence should be addressed. Tel.: 319-335-7864; Fax: 319-335-7330; E-mail: nikolai-artemyev@uiowa.edu.

‡ Recipient of NIDDK Postdoctoral Training Grant Fellowship DK-07759-03.

§ Established Investigator of the American Heart Association.

[1] Abbreviations: AGS3, activator of G-protein signaling; BC, 3-(bromoacetyl)-7-diethylaminocoumarin; GAP, GTPase activating protein; GDI, guanine nucleotide dissociation inhibitor; GEF, guanine nucleotide exchange factor; GPCR, G-protein coupled receptor; GPR-motif, G-protein regulatory motif; GST, glutathione *S*-transferase; GTPγS, guanosine 5′-*O*-(3-thiotriphosphate); Pcp2, Purkinje cell protein-2.

10.1021/bi015708k CCC: $22.00
Published on Web 12/11/2001

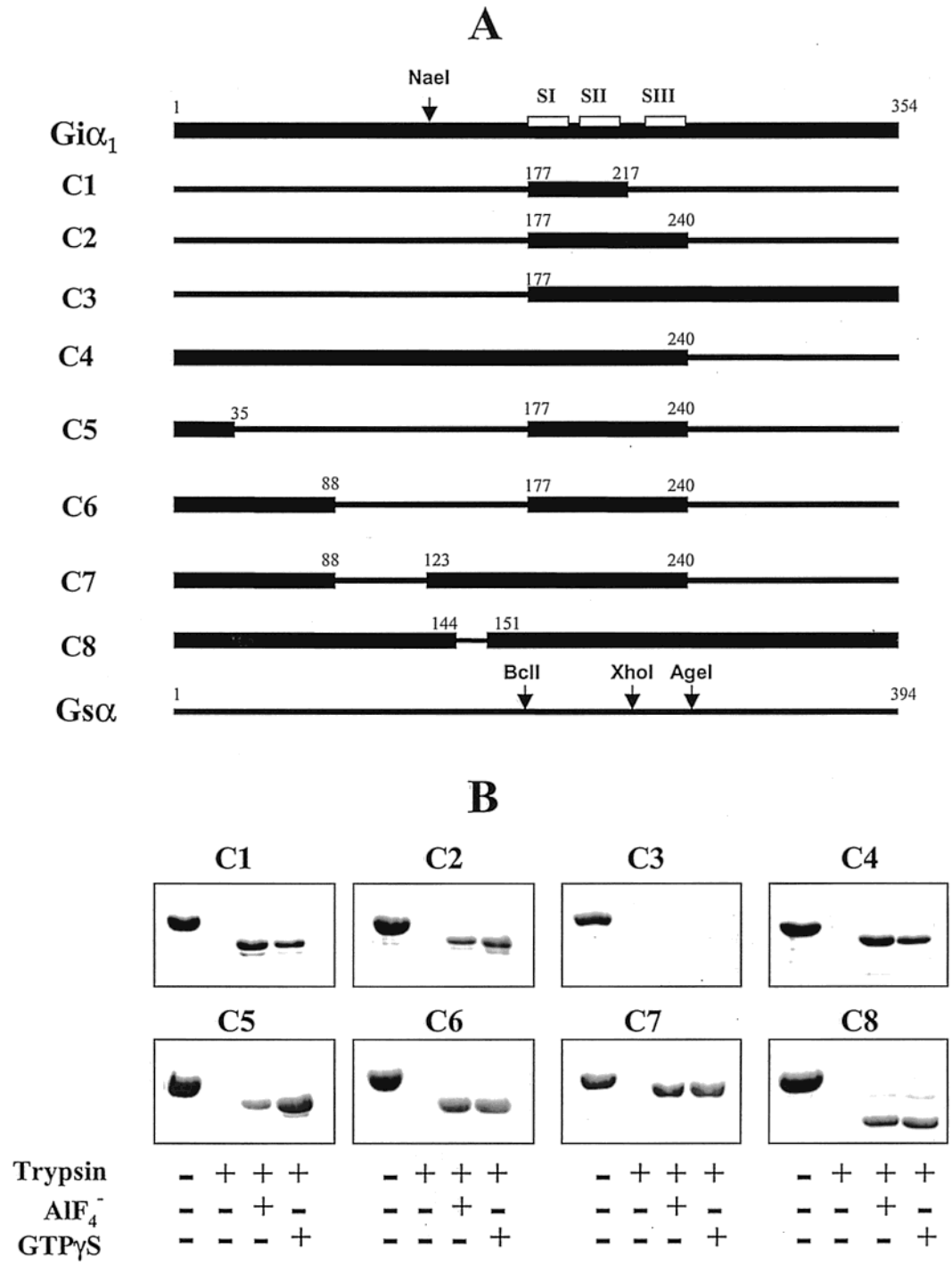

FIGURE 1: Giα$_1$/Gsα chimeras. (A) Schematic representation of the Giα$_1$/Gsα chimeras. The conformational switches SI, SII, and SIII are shown. Restriction sites that were utilized in the cloning of chimeras are denoted. The numbers above chimeras indicate the junction points of Giα$_1$ and Gsα using the sequence of Giα$_1$. (B) Trypsin-protection test for chimeric Gα subunits. SDS−polyacrylamide gels (12%) were stained with Coomassie Blue. Chimeras (1 mg/mL) were treated with trypsin (25 μg/mL) for 15 min at 25 °C in the presence of 10 μM GDP, 10 μM GDP/30 μM $AlCl_3$/10 mM NaF, or 10 μM GTPγS.

introduced into the Gsα cDNA using a QuikChange kit (Stratagene): the *Bcl*I site (codons for Ser^{193}−Gln^{195}), the *Xho*I site (codons for Ser^{250}−Ser^{252}), and the *Age*I site (codons Asn^{264}−Leu^{266}) (Figure 1A). To construct chimeras C1−C4 (Figure 1A), Giα$_1$ cDNA fragments between the *Bcl*I and *Xho*I (C1), *Bcl*I and *Age*I (C2), *Bcl*I and *Hin*dIII (C3), and *Nco*I and *Age*I (C4) sites were PCR-amplified and subcloned into the pHis$_6$-Gsα cut with appropriate restriction enzymes. Chimeras C5 and C6 (Figure 1A) were generated using the C2 construct as a template and the "megaprimer" method of site-directed mutagenesis (*16*). To generate C7 (Figure 1A), a PCR amplification of C6 was performed with an *Nco*I-flanked primer and a reverse 5′-phosphorylated primer coding for residues 139−145 of Gsα and residues 123−124 of Giα$_1$ at the 5′-end. The fragment was ligated into the C4 construct digested with *Nco*I and *Nae*I. Chimera C8 (Figure 1A) was prepared by PCR amplifications of two Giα$_1$ cDNA fragments. The first fragment was amplified with a forward primer containing a *Nco*I site and a 5′-phosphorylated reverse primer coding for the Arg^{144}→Asn substitu-

tion. The second fragment was amplified with a forward 5′-phosphorylated primer coding for the Asn^{149}→Ile and Ser^{151}→Cys substitutions and a reverse primer containing a *Hin*dIII site. The fragments were ligated and subcloned into the pHis$_6$ vector. Automated DNA sequencing at the University of Iowa DNA Core Facility confirmed the structure of all generated chimeras. The bacterial strain GM2163 was utilized to obtain nonmethylated DNA necessary for *Bcl*I digestion.

Expression and Purification of Chimeric Gα Subunits. For protein expression, 1 L of 2×TY medium was inoculated with a single colony of transformed BL21(DE3) cells. Protein expression was induced at $A_{600} \sim 0.5$ by the addition of 30 μM isopropyl-β-D-thiogalactopyranoside. After an incubation for 16 h at 25 °C, cells were pelleted and processed immediately or stored frozen at −80 °C. Purification was performed using His·Bond resin (Novagen) as described before (*14*). A typical yield of >90% pure protein was 20 mg/L of culture.

Cloning and Expression of GPR-Proteins. cDNA corresponding to residues 463−650 of the rat AGS3 and coding for all four GPR motifs (*5*) was PCR-amplified with primers containing the *Nde*I and *Bam*HI sites and subcloned into the pET15b vector for expression of a His$_6$-tagged AGS3GPR as described (*11*). The His$_6$- and GST-tagged human Pcp2 proteins were made as described (*11*).

Trypsin-Protection Assay. Purified chimeras C1−C8 (∼1 mg/mL) were incubated for 1 h at 25 °C in 20 mM HEPES buffer, pH 8.0, containing 130 mM NaCl and 8 mM $MgCl_2$ (buffer A) in the presence of either 10 μM GDP, 10 μM GTPγS, or 10 μM GDP, 30 μM $AlCl_3$, and 10 mM NaF. Trypsin was added at a concentration of 25 μg/mL followed by 15 min incubation at 25 °C. The proteolysis was stopped by the addition of SDS-sample buffer and instantaneous heating to 100 °C for 5 min.

The GST-Pcp2 Pull-Down Assay. Giα$_1$, Gsα, and chimeras C1−C8 (1 μM) were incubated for 10 min at 25 °C in 100 μL of buffer A containing either 10 μM GDP or 10 μM GDP, 30 μM $AlCl_3$, and 10 mM NaF followed by addition of 4 μM GST-Pcp2 and further incubation for 20 min at 25 °C. The proteins were then mixed with glutathione−agarose beads (10 μL bed volume) for 20 min. The beads were spun down and washed 4 times with 1 mL of buffer A containing 10 μM GDP or 10 μM GDP, 30 μM $AlCl_3$, and 10 mM NaF. Bound proteins were eluted with SDS-sample buffer and applied on 12% SDS-gels.

GTPγS Binding Assay. Giα$_1$, Gsα, and chimeras C1−C8 (0.2 μM) alone, or mixed with the indicated concentrations of His$_6$-Pcp2 or His$_6$-AGS3GPR, were incubated for 3 min at 25 °C in buffer A containing 10 μM GDP and 10 mM DTT. The binding reactions were initiated with additions of 5 μM [^{35}S]GTPγS (5 Ci/mmol). Aliquots (20 μL) were withdrawn from the binding mixtures and passed through Whatman cellulose nitrate filters (0.45 μm). The filters were washed 3 times with 1 mL of ice-cold buffer A, dissolved in a scintillation cocktail 3a70B (RPI Corp.), and counted. Background GTPγS binding in the absence of Gα was subtracted from the binding data. The GTPγS binding data were fit to the equation: GTPγS bound (%) = $100 \times (1 - e^{-kt})$.

A Fluorescence Assay of Pcp2BC Binding to Gα Subunits. His$_6$-Pcp2 was labeled at a single cysteine residue (Pcp2Cys6) with the environmentally sensitive florescent probe BC as described before (*11*). Using $\epsilon_{445} = 53\,000$ for BC, the incorporation of BC into Pcp2 was greater than 0.8 mol/mol. Fluorescence assays were performed on a F-2000 fluorescence spectrophotometer (Hitachi) in 1 mL of 20 mM HEPES buffer, pH 7.6, containing 100 mM NaCl and 10 mM $MgCl_2$. Fluorescence of 40 nM Pcp2BC was monitored before and after additions of increasing concentrations of Gα subunits with excitation at 445 nm and emission at 495 nm. The binding specificity was confirmed using a competitive displacement of Pcp2BC with unlabeled Pcp2.

Miscellaneous Procedures. Protein concentrations were determined by the Bradford method using IgG as a standard (*17*). SDS−PAGE was performed by the Laemmli method (*18*). The experimental data were fit using the nonlinear least-squares criteria method and the GraphPad Prizm (v.2) software. Data are shown as the mean ± SE of at least three experiments.

RESULTS

Role of Giα Switch Regions in the Interaction with GPR-Proteins. The design of initial Giα$_1$/Gsα chimeras to probe Giα/GPR-protein interaction regions was based on the preferential binding of GPR-proteins to GiαGDP. The conformational selectivity of GPR-proteins suggests a potential role of the Giα switch regions in the interaction. Accordingly, the switch I and II regions, or all three switch regions of Giα$_1$, were replaced with Gsα in chimeras C1 and C2, respectively (Figure 1A). Both chimeras were correctly folded and protected from a tryptic cleavage in the presence of GTPγS or AlF_4^- (Figure 1B). C1 and C2 displayed drastically different rates of GTPγS binding. The initial GTPγS binding rate to C1 was similar to that of Gsα [0.024 mol of GTPγS/(min·mol)] (Figure 2) (*9*). In contrast, the initial rate of [^{35}S]GTPγS binding to C2 was too fast for accurate determination (>5 min^{-1}), suggesting a very rapid release of GDP from the chimeric protein (Figure 2). Even when added at high concentrations (20 μM), AGS3GPR and Pcp2 failed to inhibit the GTPγS binding to either C1 or C2 (Figure 2). Consistent with the lack of the inhibitory effect, GST-Pcp2 did not coprecipitate C1 and C2 in the GST pull-down experiments (Figure 3). However, a more sensitive fluorescence assay of the interaction showed a relatively weak binding of Pcp2BC to C1 or C2. Using this assay, the K_d values for C1 (1.0 μM) and C2 (0.8 μM) were higher and the F/Fo_{max} values (1.66 for C1, 2.6 for C2) were significantly lower than the K_d (0.34 μM) and F/Fo_{max} values (6.3) for Giα$_1$ (Figure 4). From the fluorescence assay, it appears that C1 and C2 have a ∼3-fold lower affinity for Pcp2 in comparison to Giα$_1$. However, the pull-down assays indicate that the difference might be even greater (Figure 3). In control experiments, the addition of Gsα produced only a very small linear increase in the fluorescence of Pcp2BC (Figure 4B). The lack of hyperbolic dependence in this fluorescence increase might be indicative of the nonspecific background signal. The data on C1 and C2 show that the switch regions of Giα$_1$ modestly contribute to the interaction with GPR-proteins, but are not sufficient for the latter to act as GDIs.

The Helical Domain of Giα$_1$ Contains an Important Determinant(s) for GPR-Protein Recognition. The following

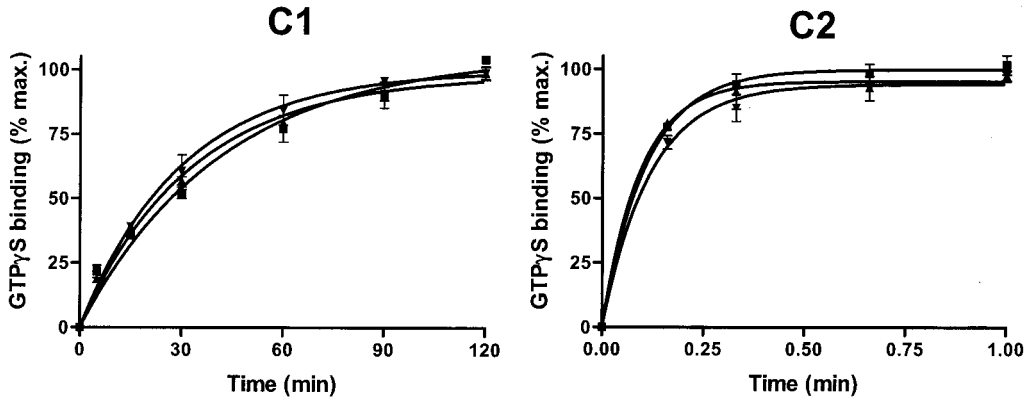

FIGURE 2: Effects of AGS3GPR and Pcp2 on the kinetics of GTPγS binding to chimeras C1 and C2. The binding of GTPγS to chimeric Giα_1/Gsα proteins (0.2 μM) in the absence (■) or presence of 20 μM His6-tagged AGS3GPR (▼) or Pcp2 (▲) was initiated by the addition of 5 μM [^{35}S]GTPγS. Gα-bound GTPγS was counted by withdrawing aliquots at the indicated times and passing them through cellulose nitrate filters (0.45 μm). The initial rates of GTPγS binding to C1 [mol of GTPγS/(min·mol)] are as follows: 0.024 ± 0.002 (■), 0.033 ± 0.003 (▼), and 0.030 ± 0.003 (▲). Initial rates of GTPγS binding to C2 are >5 min^{-1}.

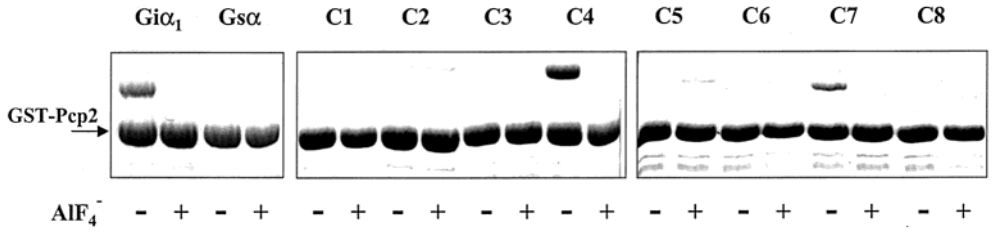

FIGURE 3: Binding of GST-Pcp2 to Gα subunits. SDS−polyacrylamide gels (12%) stained with Coomassie Blue. Gα proteins bound to GST-Pcp2 were pulled-down using glutathione−agarose beads as described under Experimental Procedures in the absence or presence of AlF_4^-. Bound proteins were eluted with SDS-sample buffer and analyzed by electrophoresis.

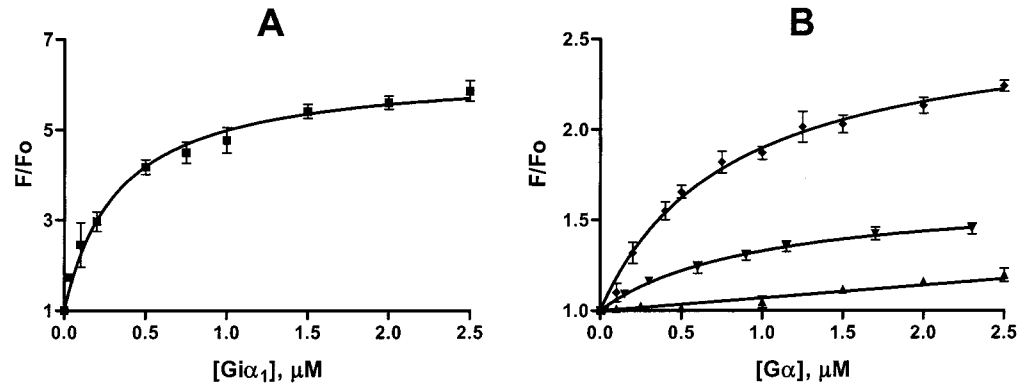

FIGURE 4: Binding of Giα1, C1, C2, and Gsα to Pcp2BC. The relative increase in fluorescence (F/Fo) of Pcp2BC (40 nM) (excitation at 445 nm, emission at 495 nm) was determined following the addition of increasing concentrations of Gα proteins. The binding curve characteristics are as follows: (A) Giα_1, K_d = 0.34 ± 0.02 μM, F/Fo_{max} = 6.3; and (B) C1, K_d = 1.00 ± 0.12 μM, F/Fo_{max} = 1.66 (▼); C2, K_d = 0.80 ± 0.06 μM, F/Fo_{max} = 2.6 (◆), and Gsα (▲).

two chimeric Gα subunits, C3 and C4, were generated to determine whether an additional GPR interaction site(s) is (are) located N- or C-terminally to the switch regions (Figure 1A). The trypsin-protection assay revealed that C3 was not protected from tryptic cleavage in the presence of GDP·AlF_4^- or GTPγS, whereas C4 displayed a normal pattern of tryptic fragments (Figure 1B). However, both chimeras were functional in the GTPγS binding assay. The initial rate of GTPγS binding for C3 (1.21 min^{-1}) (not shown) was ~30 times faster than that for C4 (0.039 min^{-1}) (Figure 5). The GPR-proteins did not notably affect the kinetics of GTPγS binding to C3 (not shown). In contrast, AGS3GPR and Pcp2 markedly inhibited the rate of GTPγS binding to C4 (Figure 5A,B). The IC_{50} values for the inhibitory effects of AGS3 (0.49 μM) and Pcp2 (0.63 μM) on C4 were only ~4-fold higher than the respective IC_{50} values for the GPR effects on Giα_1 (Figure 5C and refs *9*, *11*). A strong interaction of C4 with Pcp2 was confirmed in the GST-Pcp2 pull-down assay (Figure 3), and in the fluorescence binding assay using Pcp2BC (Figure 5D). The calculated K_d (0.32 μM) and maximal F/Fo (4.7) values for the binding of C4 to Pcp2BC were not significantly different from those for Giα_1 (Figure 4A). These results suggest that the N-terminal half of Giα_1 contains an essential GPR interaction site(s) that allow(s) GPR to inhibit the nucleotide exchange.

GPR-proteins compete with G$\beta\gamma$ subunits for binding to GαGDP (*10*, *11*). The N-terminal helix of Gα is one of the major G$\beta\gamma$ binding sites, and, therefore, might have been a site of competition between GPR and G$\beta\gamma$. Chimera C5 (Figure 1A), containing the 35 N-terminal residues and the

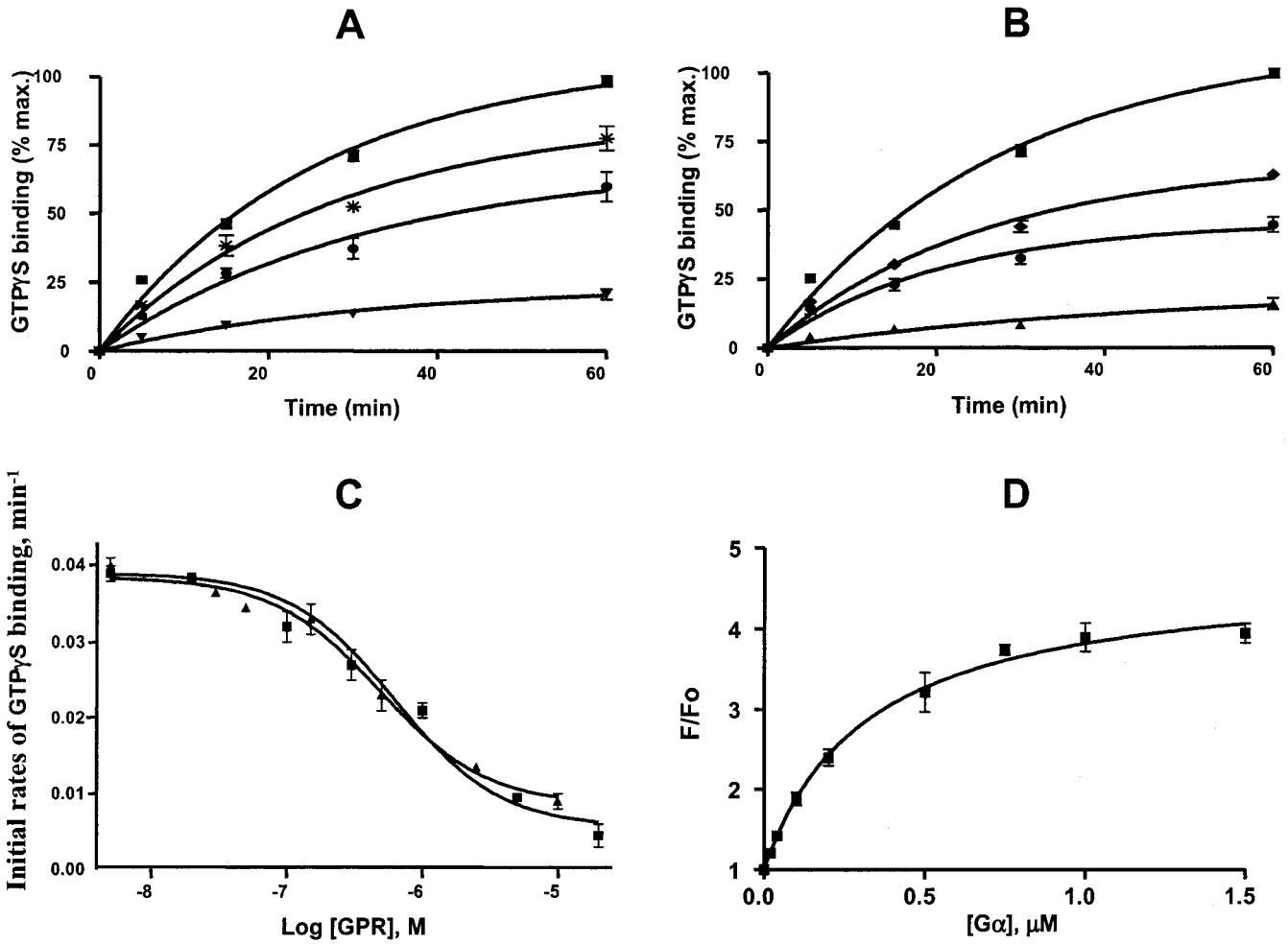

FIGURE 5: Interactions of AGS3GPR and Pcp2 with chimera C4. The binding of GTPγS to C4 (0.2 μM) in the absence (■) or presence of AGS3GPR (A) and Pcp2 (B) [0.15 μM (*), 0.3 μM (◆), 1 μM (●), 10 μM (▼), 20 μM (▲)] was initiated by the addition of 5 μM [^{35}S]GTPγS. C4-bound GTPγS was counted by withdrawing aliquots at the indicated times. The initial rates of GTPγS binding [mol of GTPγS/(min·mol)] are as follows: 0.039 ± 0.004 (■), (A) 0.033 ± 0.003 (*), 0.023 ± 0.002 (●), 0.009± 0.001 (▼); (B) 0.027 ± 0.004 (◆), 0.021 ± 0.003 (●), 0.005 ± 0.001 (▲). (C) The initial rates of GTPγS binding to C4 are plotted as a function of AGS3GPR (▲) or Pcp2 (■) concentrations. The IC_{50} values (μM) are 0.49 ± 0.04 (▲) and 0.63 ± 0.05 (■). (D) The relative increase in fluorescence (*F/F*o) of Pcp2BC (40 nM) was determined following the addition of increasing concentrations of C4. The binding curve characteristics are $K_d = 0.32 \pm 0.03$ μM and $F/Fo_{max} = 4.7$.

switch regions of Giα_1, was generated to probe a possible involvement of the Giα_1 N-terminus in the binding to GPR-proteins. Similarly to C2, the kinetics of GTPγS binding to C5 were very fast with the initial rate exceeding 5 min^{-1} (not shown). No inhibition of GTPγS binding to C5 by AGS3GPR and Pcp2 was detected (not shown). In agreement with this observation, the pull-down assay showed no coprecipitation of C5 with GST-Pcp2 (Figure 3).

The rates of GTPγS binding, and hence the rates of GDP release, were extremely high for two chimeras, C2 and C5, indicating that these proteins can readily lose GDP. However, the high GTPγS binding rates and the lack of GPR binding to such chimeras were most likely not due to the loss of GDP or gross conformational changes. The GTPγS binding and pull-down assays were carried out in the presence of 10 μM GDP, the same nucleotide concentration as used in the trypsin-protection assay. The trypsin cleavage of C2 and C5 in the presence of GDP produced proteolytic fragments of ~20 kDa that are characteristic of tryptic digests of GDP-bound Gα subunits (not shown) (*19*). The trypsin-protection assay in the presence of GDP and AlF_4^- (Figure 1B) also suggests that C2 and C5 subunits bind GDP under our experimental conditions and have proper overall folding. The lack of functional coupling of the GPR-proteins to C5 together with the sequence identity between the Giα_1 residues 36−53 and Gsα residues 43−60 indicated that the remaining GPR recognition domain is localized within the helical domain of Giα_1.

Identification of a Giα/GPR Interaction Site within the Helical Domain of Giα. To further delineate the GPR interaction region within the helical domain of Giα_1, a larger N-terminal sequence of Giα_1, Giα_1-1−88, was replaced in C2 to produce chimera C6 (Figure 1A). This chimera was functionally folded as judged from the trypsin-protection assay (Figure 1B). The initial rate of GTPγS binding to C6 was relatively fast (0.44 min^{-1}) (Figure 6). No inhibition of GTPγS binding to C6 was observed in the presence of 20 μM Pcp2 or AGS3GPR (Figure 6). Furthermore, C6 did not coprecipitate with GST-Pcp2 in the pull-down assay (Figure 3). In comparison to C6, chimera C7 contained Giα_1 residues 123−177 from the helical domain (Figure 1A). In contrast to C6, C7 had a lower GTPγS binding rate (0.066 min^{-1}) (Figure 7). AGS3GPR and Pcp2 effectively inhibited GTPγS binding to C7 with IC_{50} values of 0.5 and 0.65 μM,

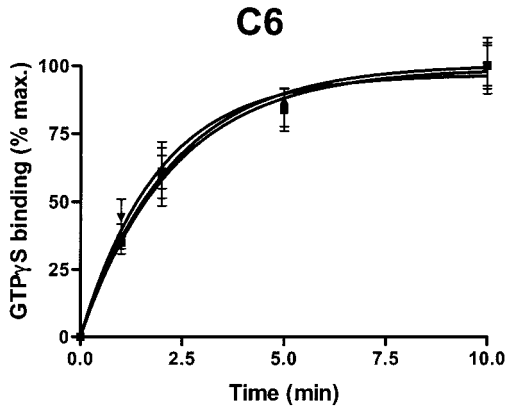

FIGURE 6: Effects of AGS3GPR and Pcp2 on the kinetics of GTPγS binding to chimera C6. The binding of GTPγS to C6 (0.2 μM) in the absence (■) or presence of 20 μM AGS3GPR (▼) and Pcp2 (▲) was initiated by the addition of 5 μM [^{35}S]GTPγS. The initial rates of GTPγS binding [mol of GTPγS/(min·mol)] are 0.44 ± 0.03 (■), 0.50 ± 0.05 (▼), and 0.43 ± 0.04 (▲).

respectively (Figure 7A−C). Efficient functional interaction of C7 with Pcp2 was confirmed in the GST pull-down and Pcp2BC fluorescence assays (Figures 3 and 7D). Using the fluorescence binding assay, the affinity of C7 for Pcp2BC (K_d = 0.4 μM) was comparable to that of Giα_1 (Figure 4A). The analysis of chimeric Gα subunits C1−C7 indicated a GPR binding site(s) within the switch regions and a second site within Giα_1-123−176, which is important for the GDI activity. The crystal structures of Giα show that within Giα_1-123−176, only residues 144−151 are surface-exposed on the same side of Giα as the switch regions (*20*, *21*). Furthermore, this face of Gα is a probable route for the release of GDP (*20*−*23*). These considerations were taken into account in designing chimera C8, which was derived from Giα_1 by replacing residues 144−151 with Gsα-specific residues. Only three residues in C8 are different from the wild-type Giα_1: Arg^{144}→Asn, Asn^{149}→Ile, and Ser^{151}→Cys. C8 was correctly folded as evidenced by the trypsin-protection assay (Figure 1B). The rate of GTPγS binding to C8 was significantly higher (0.28 min^{-1}) than that to Giα_1 (Figure 8A and refs *9*, *11*). AGS3GPR and Pcp2 at 20 μM concentration did not change the kinetics of GTPγS binding to C8 (Figure 8A), and the pull-down assay confirmed the impairment of C8 binding to GST-Pcp2 (Figure 3). The sensitive fluorescence binding assay detected a weak residual interaction between C8 and Pcp2BC (K_d = 2.4 μM, F/Fo_{max} = 3.1) (Figure 8B).

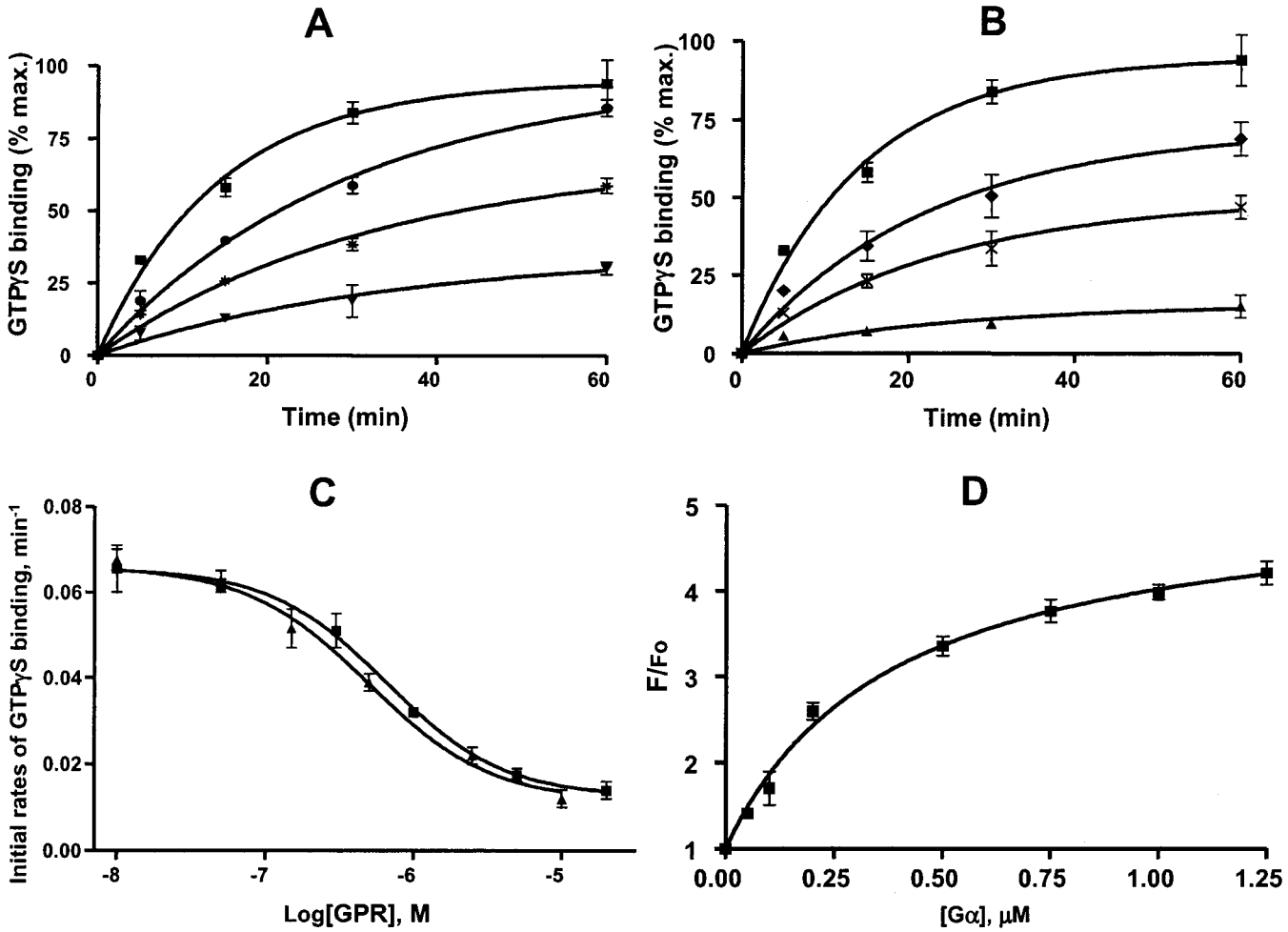

FIGURE 7: Interactions of AGS3GPR and Pcp2 with chimera C7. The binding of GTPγS to C7 (0.2 μM) in the absence (■) or presence of AGS3GPR (A) and Pcp2 (B) [0.3 μM (◆), 0.5 μM (●), 1 μM (×), 2.5 μM (*), 10 μM (▼), 20 μM (▲)] was initiated by the addition of 5 μM [^{35}S]GTPγS. The initial rates of GTPγS binding [mol of GTPγS/(min·mol)] are 0.066 ± 0.006 (■), (A) 0.035 ± 0.003 (●), 0.021 ± 0.002 (*), 0.012 ± 0.001 (▼); (B) 0.037 ± 0.004 (◆), 0.030 ± 0.003 (×), 0.006 ± 0.001 (▲). (C) The initial rates of GTPγS binding to C7 are plotted as functions of AGS3GPR (▲) or Pcp2 (■) concentrations. The IC_{50} values (μM) are 0.50 ± 0.04 (▲) and 0.65 ± 0.05 (■). (D) The relative increase in fluorescence (F/Fo) of Pcp2BC was determined following the addition of increasing concentrations of C7. The binding curve characteristics are K_d = 0.40 ± 0.03 μM and F/Fo_{max} = 5.2.

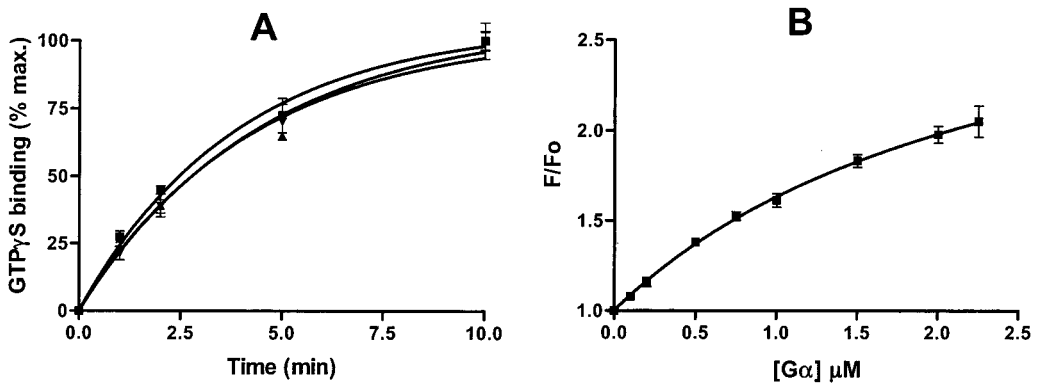

FIGURE 8: Interactions of AGS3GPR and Pcp2 with chimera C8. (A) Effects of AGS3GPR and Pcp2 on the kinetics of GTPγS binding to chimera C8. The binding of GTPγS to C8 (0.2 μM) in the absence (■) or presence of 20 μM AGS3GPR (▼) and Pcp2 (▲) was initiated by the addition of 5 μM [^{35}S]GTPγS. The initial rates of GTPγS binding [mol of GTPγS/(min·mol)] are 0.28 ± 0.02 (■), 0.24 ± 0.01 (▼), and 0.26 ± 0.02 (▲). (B) The relative increase in fluorescence (*F*/*F*o) of Pcp2BC (40 nM) was determined following the addition of increasing concentrations of C8. The binding curve characteristics are K_d = 2.4 ± 0.3 μM and F/Fo_{max} = 3.1.

DISCUSSION

GTP binding proteins are key cellular signaling molecules that switch between two main conformations: inactive, GDP-bound; or activated, GTP-bound. A GTP binding protein is activated when the bound GDP is released and exchanged for GTP. Intrinsic GTPase activity inactivates G-proteins by converting the bound GTP to GDP. Three groups of protein modulators control the activation/inactivation cycle of small monomeric GTPases: guanine nucleotide exchange factors (GEFs), guanine nucleotide dissociation inhibitors (GDIs), and GTPase-activating proteins (GAPs) (*24*). GPCRs play a role of functional analogues of GEFs for heterotrimeric GTP binding proteins (G-proteins). A ligand- or signal-activated GPCR induces GDP release from a Gα subunit of a cognate G-protein, followed by binding of GTP and dissociation of G$\beta\gamma$. Recent reports suggest that in addition to GPCRs, other G-protein modulators, such as AGS1, exhibit a GEF-like activity toward G-proteins (*25*). The mechanism of AGS1 GEF activity is not yet known. RGS proteins, in some instances in conjunction with G-protein effectors, serve as GAPs for G-proteins (*26*−*28*). Although the functional parallels between modulators of monomeric GTPases and heterotrimeric G-proteins are evident, the molecular mechanisms of GPCRs and RGS-proteins are quite different from those of their functional GEF and GAP counterparts. A comparison of G$\beta\gamma$ function to that of GDI is more intricate. G$\beta\gamma$ subunits reduce spontaneous nucleotide exchange on Gα subunits by inhibiting the release of GDP. However, in contrast to GDIs, which antagonize the action of GEFs, G$\beta\gamma$ subunits are absolutely essential for the activation of G-proteins by GPCRs. Furthermore, GPCRs might directly utilize G$\beta\gamma$ to promote dissociation of GDP from Gα (*29*). A novel group of G-protein regulators containing the GPR motifs may represent "true" GDIs for G-proteins. Not only have GPR-proteins been shown to block dissociation of GDP from Gα subunits of the Gi family, but they are also capable of inhibiting G-protein activation by GPCRs (*8*, *9*). The GPR-protein binding sites on Gα subunits as well as the mechanism of GDI activity of GPR-proteins have been the focus of this study. We took advantage of the fact that known GPR-proteins do not interact with Gsα, and constructed a series of Giα/Gsα chimeras. The functional analysis of these chimeras demonstrated that the Giα switch regions participate in binding to GPR-proteins. This finding is consistent with the preferential recognition by GPR-proteins of a GDP-bound conformation of Gα subunits of the Giα family. However, the binding of chimeric Gα containing only the Giα switch regions to GPR-proteins was much weaker than that of the wild-type Giα. More importantly, the presence of Giα switch regions was not sufficient for GPR-proteins to act as GDIs. An additional site, Giα_1-144−151 (αD−αE loop), critical for the high-affinity functional interaction between Giα and a GPR-protein, has been identified within the helical domain. A replacement of a Gsα-specific sequence corresponding to Giα_1-144−151 into Giα abolished functional coupling of GPR-proteins to the chimeric Gα-subunit. Significantly, Giα_1-144−151 includes several residues making important interdomain contacts, particularly with the switch III region. Arg^{144} and Gln^{147} form direct or water-mediated contacts with Asp^{231}, Val^{233}, and Arg^{242} from the switch III loop in the GTPγS-bound conformation of Giα (*20*, *21*). In the GiαGDP structure, the switch III loop is destabilized and—with the exception of the Arg^{144}/Asp^{231} contact—the helical domain/switch III interactions are disrupted (*21*). Similar αD−αE loop/switch III contacts are seen in the structure of GtαGTPγS, and remain largely intact in GtαGDP (*22*, *23*). However, the conformational change in switch III of Gtα induces a change in position of Gtα-143−145 (*23*). The short segment ^{143}QLN^{145} in Gtα (^{147}QLN^{149} in Giα_1) is the only site in the helical domain of Gtα that differs in GtαGTPγS and GtαGDP (*23*). Interestingly, Giα_1Asn^{149} (GtαAsn^{145}) is substituted by an Ile residue in Gsα. Two other residues within Giα_1-144−151 are different between Giα and Gsα: Arg^{144}/Asn and Ser^{151}/Cys. The lack of matching helical domain/switch III contacts most likely explains high rates of GTPγS binding observed in a number of tested chimeric Gα subunits. A loss of the interdomain contact involving Arg^{144} and Leu^{232} was shown to significantly increase the rate of GDP dissociation from Giα_1 (*30*). In addition to the regulation of GDP release and recognition of GPR-proteins, the αD−αE loop/switch III coupling appears to be essential for a GPCR-mediated activation of G-proteins (*31*).

The Giα_1-144−151 region can contribute to the GPR/Giα interaction in two ways. Since the helical domain/switch III interface is conformation-sensitive, it probably—together with the switch I−II regions—forms a GPR binding surface. In

addition, $Gi\alpha_1$-144−151 may directly interact with GPR-motifs. The $Gi\alpha_1$-144−151 and switch III constitute a part of a deep nucleotide binding cleft between the helical and GTPase domains. Binding of a GPR-protein to the $Gi\alpha_1$-144−151/switch III region and switches I/II not only would stabilize the GDP-bound conformation of Giα but also is likely to physically block GDP release. The latter mechanism is consistent with the observation that GPR-proteins inhibit AlF_4^- -induced activation of GiαGDP (*12*, *13*).

The helical domain (I1) and switch III (I2) are two of the four insert regions (I1−I4) that are unique for heterotrimeric G-protein α subunits (*22*). Therefore, the mechanism of GDI activity of GPR-proteins would most likely be different from that of GDIs for monomeric GTPases such as RhoGDI. The RdoGDI/Cdc42 structure revealed the critical interactions of the amino-terminal arm of RdoGDI with the switch I and II regions of Cdc42 that inhibit GDP release via stabilization of Mg^{2+} coordination and bound GDP (*32*). In contrast, the binding of a GPR-protein to switches I and II of Giα appears to be insufficient for the GDI activity.

Overall, our data suggest the GDI activity of the GPR-protein involves a novel mechanism that is different from that of $G\beta\gamma$ subunits. Unlike $G\beta\gamma$ subunits, GPR-proteins appear to utilize the helical domain/switch III interface to inhibit the release of GDP. The inhibition probably involves a physical blockade of the GDP escape route.

REFERENCES

1. Gilman, A. G. (1987) *Annu. Rev. Biochem. 56*, 615−649.
2. Bourne, H. R. (1997*) Curr. Opin. Cell Biol. 9*, 134−142.
3. Lefkowitz, R. L. (1998) *J. Biol. Chem. 273*, 18677−18680.
4. Hamm, H. E. (1998) *J. Biol. Chem. 273*, 669−672.
5. Takesono, A., Cismowski, M. J., Ribas, C., Bernard, M., Chung, P., Hazard, S., III, Duzic, E., and Lanier, S. M. (1999) *J. Biol. Chem. 274*, 33202−33205.
6. Siderovski, D. P., Diverse-Pierluissi, M. A., and De Vries, L. (1999) *Trends Biochem. Sci. 24*, 340−341.
7. Ponting, C. P. (1999) *J. Mol. Med. 77*, 695−698.
8. Peterson, Y. K., Bernard, M. L., Ma, H., Hazard, S., III, Graber, S. G., and Lanier, S. M. (2000) *J. Biol. Chem. 275*, 33193−33196.
9. Natochin, M., Lester, B. R., Peterson, Y. K., Bernard, M. L., Lanier, S. M., and Artemyev, N. O. (2000) *J. Biol. Chem. 275*, 40981−40985.
10. Bernard, M. L., Peterson, Y. K., Chung, P., Jourdan, J., and Lanier, S. M. (2001) *J. Biol. Chem. 276*, 1585−1593.
11. Natochin, M, Gasimov, K. G., and Artemyev, N. O. (2001) *Biochemistry 40*, 5322−5328.
12. De Vries, L., Fischer, T., Tronchere, H., Brothers, G. M., Strockbine, B., Siderovski, D. P., and Farquhar, M. G. (2000) *Proc. Natl. Acad. Sci. U.S.A. 97*, 14364−14369.
13. Kimple, R. J., De Vries, L., Tronchere, H., Behe, C. I., Morris, R. A., Farquhar, M. G., and Siderovski, D. P. (2001) *J. Biol. Chem. 276*, 29275−29281.
14. Skiba, N. P., Bae, H., and Hamm, H. E. (1996) *J. Biol. Chem. 271*, 413−424.
15. Natochin, M., and Artemyev, N. O. (1998) *Biochemistry 37*, 13776−13780.
16. Sarkar, G., and Sommer, S. S. (1990) *BioTechniques 8*, 404−407.
17. Bradford, M. M. (1976) *Anal. Biochem. 72*, 248−254.
18. Laemmli, U. K. (1970) *Nature 227*, 680−685.
19. Winslow, J. W., Van Amsterdam, J. R., and Neer, E. J. (1986) *J. Biol. Chem. 261*, 7571−7579.
20. Coleman, D. E., Berghuis, A. M., Lee, E., Linder, M. E., Gilman, A. G., and Sprang, S. R.(1994) *Science 265*, 1405−1412.
21. Mixon, M. B., Lee, E., Coleman, D. E., Berghuis, A. M., Gilman, A. G., and Sprang, S. R. (1995) *Science 270*, 954−960.
22. Noel, J. P., Hamm, H. E., and Sigler, P. B. (1993) *Nature 366*, 654−663.
23. Lambright, D. G., Noel, J. P., Hamm, H. E., and Sigler, P. B. (1994) *Nature 369*, 621−628.
24. Geyer, M., and Wittinghofer, A. (1997) *Curr. Opin. Struct. Biol. 7*, 786−792.
25. Cismowski, M. J., Ma, C., Ribas, C., Xie, X., Spruyt, M., Lizano, J. S., Lanier, S. M., and Duzic E. (2000) *J. Biol. Chem. 275*, 23421−23424.
26. Koelle, M. R. (1997) *Curr. Opin. Cell Biol. 9*, 143−147
27. Berman, D. M., and Gilman, A. G. (1998*) J. Biol. Chem. 273*, 1269−1272
28. He, W., Cowan, C. W., and Wensel, T. G. (1998) *Neuron 20*, 95−102.
29. Rondard, P., Iiri, T., Srinivasan, S., Meng, E., Fujita, T., and Bourne, H. R. (2001) *Proc. Natl. Acad. Sci. U.S.A. 98*, 6150−6155.
30. Remmers, A. E., Engel, C., Liu, M., and Neubig, R. R. (1999) *Biochemistry 38*, 13795−13800.
31. Grishina, G., and Berlot, C. H. (1998) *J. Biol. Chem. 273*, 15053−15060.
32. Hoffman, G. R., Nassar, N., and Cerione, R. A. (2000) *Cell 100*, 345−356.

BI015708K